Proceedings of the 6th European Conference of the Prognostics and Health Management Society 2021 - ISBN – 978-1-936263-34-9

Hybrid Approach for Health Monitoring of Mud Motor Fleet

Dmitry Belov[1], Zhengxin Zhang[2], Wei Chen[3], Yuelin Shen[4], Samba Ba[5], Anton Kolyshkin[6], Sergio Daniel Rocchio[7], and Daniel Viassolo[8]

[1,2,3,4,6,7,8]*Schlumberger Ltd., Houston, TX, 77056, USA*

dbelov1@slb.com, zzhang02@slb.com, wchen01@slb.com, yshen@slb.com, akolyshkin@slb.com, srocchio@slb.com, dviassolo@slb.com

[5]*Schlumberger Ltd., Beijing, 100084, China*

sba@slb.com

ABSTRACT

A mud motor is a positive displacement motor (PDM) that transform the hydraulic energy of the drilling fluids into mechanical energy and enables the drill bit to cut the rock and drill a well. Mud motor failure is a common and costly issue in drilling operations. A proper prediction of the failure as well as an estimation of the remaining useful life (RUL) are essential for timely downhole mud motor maintenance and drilling optimization.

Until now, the oil and gas industry has lacked reliable procedures to monitor and maintain the health of mud motors, resulting in unnecessary maintenance and fleet management costs as well as unpredictable and costly drilling failures. This paper presents an industry-first prognostics and health management (PHM) solution, which estimates the health of the mud motor and tracks its RUL. The proposed PHM solution is suitable for real-time implementation and combines two different sterling algorithms.

It enables the estimation of the mud motor health both at the system level for the entire mud motor (system level PHM model) and at the subcomponent level via tracking of power section RUL — the most critical component of the mud motor.

The new solution for mud motor PHM was successfully verified and tested in the field. This PHM solution enables optimization of mud motor selection, drilling configuration, and maintenance operations by minimizing RUL uncertainties while facilitating rerun decisions and avoiding overmaintenance and premature retirements.

1. INTRODUCTION

Mud motor failure is a common and costly problem in drilling operations, which typically results in lower rate of penetration (ROP) and significant loss of time and money in the worst-case scenario. Until now, there were no field methods or procedures to estimate remaining useful life of mud motors in real time, and that is leading to unnecessary maintenance and repair costs (Ba, S. & Kolyshkin, A., US10139326B2). The proper predictions of mud motor failure and estimation of RUL is quite important for the optimization of the drilling process and the maximization of revenue for oil and gas service companies. In this paper, we would like to present an industry-first prognostics and health management solution, which estimates the health of the mud motor and tracks its RUL.

The proposed PHM solution combines two different algorithms for reliable prediction of possible problems with mud motors. It enables the estimation of the mud motor health both on the system level with the entire mud motor (system level PHM model) and on the subcomponent level (power section PHM model)—the most critical component of the mud motor.

The system level algorithm model leverages both surface and downhole drilling data as well as mud motor characteristic curves to compute the severity of mud motor degradation. A special mud motor degradation indicator is defined. The indicator is calculated to evaluate the degree of power section decay at each time recorded from thousands of field jobs. The trends of the degradation with respect to drilling time and drilling distance are extracted for each motor job.

The power section PHM model uses downhole measurements to estimate the RUL of the elastomer—the life-limiting component inside the power section. It is based on a high-fidelity model and uses a hybrid approach by combining a physics-based model of a power section and data-driven approaches with machine learning techniques. Machine learning methods were applied to derive a reduced order surrogate model (ROM) of power sections from the original physics-based models for real-time applications. This ROM outputs the estimation of performance and fatigue characteristics of the considered power section depending on the considered drilling conditions such as differential pressure, downhole temperature, flow rate, and mud compatibility. As the result, the model analyzes accumulative risk of fatigue failure and produces real-time health information for the power section as a percentage of the remaining lifespan.

In this paper, RUL estimation for mud motor power sections based on the combination of two independent proposed algorithms will be discussed. After starting with a quick overview of mud motors, the modelling approach for simulating power section behavior including reduce order model will be explored before exposing in detail each RUL estimation algorithm and synergic effect after their combination. In the last part of the paper, the validation scheme for all models will be revealed before the conclusion.

2. Mud motors and their applications

A mud motor is one of the key parts of downhole assembly that is placed in the drilling assembly to provide additional power to the bit while drilling as its power downhole output is still unmatched. It is used to transform the hydraulic energy of the drilling fluid into mechanical energy on the rotation shaft. Such motors are widely used for directional drilling and performance drilling applications.

A typical mud motor consists of multiple subassemblies consisting of a power section, a transmission, a bearing section, a bent housing, a drive shaft, and top subs (Tiraspolsky, 1985) The power section (PS) assembly is the most complex element where the transformation of hydraulic power into mechanical power occurs. It has two main parts—a rotor and a stator. The rotor is a moving part and is habitually made of steel, and the stator is typically a metal tube with rubber bonded inside. A typical design and parts of a power section can be seen in Figure 1.

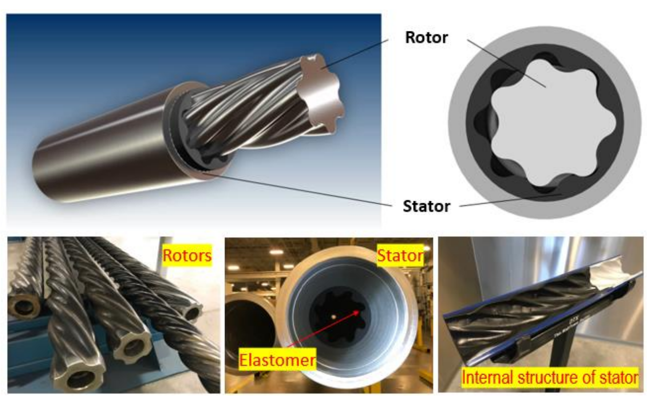

Figure 1: Mud Motor power section.

When evaluating the performance of a motor power section, it is in general necessary to refer to power curves. These power curves indicate rpm (rotation per minute) and torque output of the mud motor depending on the flow rate and differential pressure during operation. Power curves are a very important source of information for drilling engineers or directional drillers since they determine the motor usability and operating envelop. Figure 2 depicts typical power curves for different types of power sections. They show how the mud motor converts hydraulic power giving by flow rate and differential pressure to mechanical energy in terms of rotation speed and torque output.

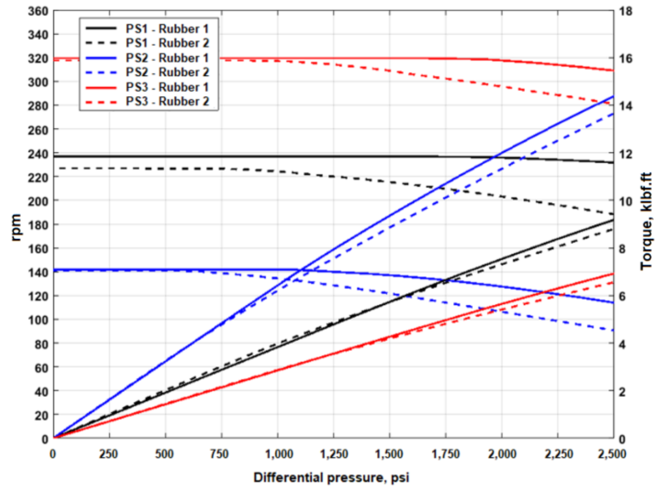

Figure 2: Power curves for different mud motor power sections.

Another important characteristic for mud motor power sections is the durability. It is often directly linked to fatigue curves. These curves enable understanding of how long the considered power section can be loaded before the elastomer inside the stator starts failing. Fatigue life depends on many parameters and it can be quite different depending on particular power sections, the operating environment or drilling conditions. Figure **3** depicts typical fatigue curves for different types of power sections.

According to statistics, the failure of power sections is the main cause of mud motor failures in more than 50% of all cases (BA, S. et al., 2016). Schlumberger internal statistics show that the other two main reasons for motor failure are transmission failure (~ 20% of all cases) and housing failure. The power section failures are most often caused by a failure of the elastomer (rubber) inside the stator, which is exposed to corrosive drilling fluid and must withstand considerable cyclic mechanical loads from the rotor and the pressure of the drilling fluid. Repetitive elastomer deformation is responsible for the growth of fatigue cracks and hysteresis heating, which ultimately can lead to elastomer chunking. Figure 4 depicts the typical damage of rubber inside PS stator due to fatigue.

Such damages to power sections in the fields are often resulting from overloading of the mud motor while drilling. The consequences of the damage can be very costly in that it significantly affects the efficiency of drilling and subsequently the cost of the well construction.

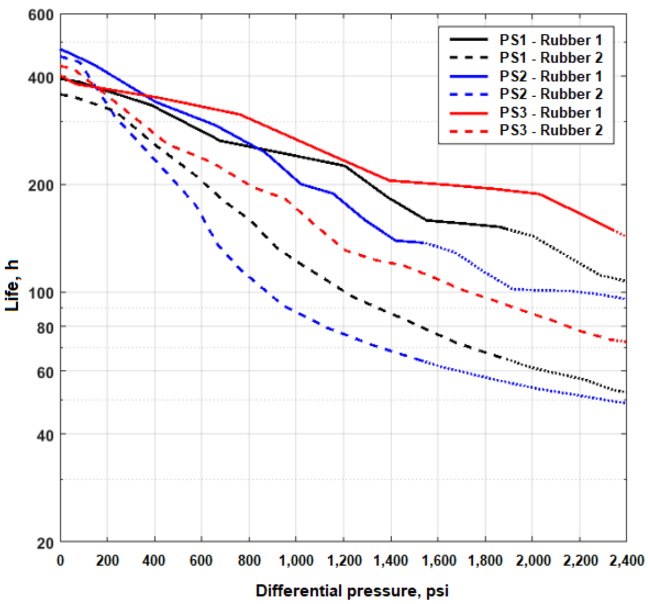

Figure 3: Fatigue curves (fatigue life vs. differential pressure) for different mud motor power sections with different rubbers.

Figure 4: Example of the failed elastomer inside power section stator due to fatigue.

The main factors affecting power section fatigue life are the mechanical design, the elastomer type, the type of drilling fluid, and the drilling conditions and environment (mud flow rate, downhole temperature, differential pressure). (BA, et al., 2016)

3. Modeling approach and ROM for power section

The relationship between motor fatigue life and operating conditions can be derived through modeling. In reality, the modelling of mud motors is not an easy task. It includes complex kinematics motion, fluid-structure interaction, geometrical, and material nonlinearity. Thus, full scale models require multiphysics simulations, involving viscoelasticity, hyperelasticity and fluid hydrodynamics (Ba et al., 2016) and consequently demand many computations resources.

Meanwhile, for health monitoring tools, the modeling results must be available instantly, i.e., in a very short time for real-time applications. Thus, it was necessary to develop a much faster reduced order model. A reduced order model (ROM) is a simplification of a high-fidelity dynamical model that preserves essential behavior and dominant effects with a satisfactory accuracy while reducing computational resources of time and storage.

To achieve the required ROM, two steps were undertaken.

At first, instead of the full-scale model, a simplified physical model of mud motor power sections was used, which is still capable of predicting its performance and reliability depending on the design and operating conditions. This model is substantially faster than the full-scale 3D model and can derive simulation results within a few minutes to a few hours, depending on the complexity of the input conditions (Kolyshkin, 2021).

Secondly, a database (using machine learning approach) was constructed on precomputed results augmented with a simple extrapolation to get scenarios which were not included in the database. That way instead of running the physical model each time and waiting minutes or hours to get results, the user would get results in milliseconds.

Regarding the physical model, two major simplifications were made:

- a set of 2D simulations is conjugated to represent dynamic behavior of stator elastomer;
- drilling fluid dynamics are reduced to a cavity network, which is connected through gaps, and there is no mechanical interaction between the fluid and the elastomer.

The first assumption is based on the periodicity of power section geometry and the fact that due to the rotor motion inside stator, each stator cross section is dynamically equal to another. Assuming small rotor and stator deformation in addition to the periodicity (Figure 5), the full power section geometry could be reduced to just one pitch length.

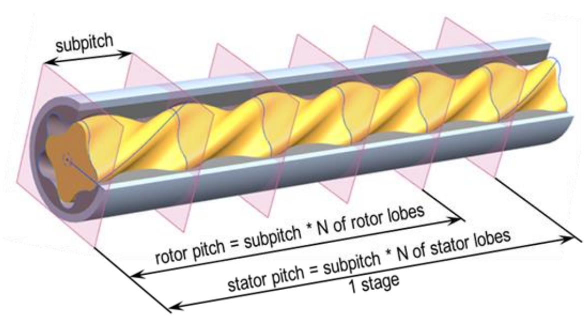

Figure 5: Power section geometry periodicity.

Moreover, within a pitch, each 2D cross section is identical as well. While the moving rotor is taking all possible positions inside the stator (Figure 6), all cross sections undergo the same deformation cycle, but shifted in time. The shift in time is proportional to the distance between them and the motion frequency.

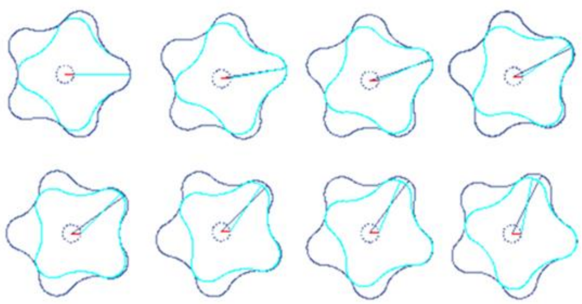

Figure 6: Relative rotor position in different cross sections.

Furthermore, the stators and rotors of mud motor power sections are normally designed to have identical lobes. So, each lobe of multilobe stator undergoes exactly the same deformation cycle as any other as well. We can effectively use this feature to increase the time resolution of the deformation cycle.

Thus, the model treats the power section as if the geometry, the displacements, the deformation, and the forces follow the same cycle for every lobe in all cross sections. Assuming that the deformation in the direction of the power section axis is substantially smaller than in the perpendicular directions, which is confirmed by 3D modeling, we can perform 2D modeling for several orientations of the rotor and stator, then derive full deformation cycle and use it to reconstruct 3D geometry. This approach is anticipated to be very relevant in the middle of the power section, however, it may result in some potentially higher deviations at both ends.

The physical model takes as input: power section geometry, elastomer properties, interference fit, downhole temperature, flow rate. The simulation results include pressure, torque, rpm, elastomer fatigue life in hours, bonding stress or debonding energy, maximum elastomer temperature due to hysteresis heating, and certain others.

For example, Figure 2 depicts the simulation results for performance curves, which link together flow rate, differential pressure, rotation speed, and torque. This type of data is important as inadequate motor performance not only compromises the drilling speed and wellbore quality, but may cause the failures for various BHA components, even not directly related to mud motors.

On a higher level of abstraction, the physical model could be considered as an operator transforming the *n*-dimensional vector X, containing n input parameters, to m-dimensional vector Y of output results:

$$f: X \rightarrow Y \quad (1)$$

The operator f involves non-linear FEA and, thus, it has relatively high computation cost. Replacing it with a reduced order model by using machine learning on the simulated results (Bataineh & Marler, 2017) yields to much faster computation time. A general scheme for the development of the motor engine using machine learning approach is presented in Figure **7**; a supervised learning technique is used.

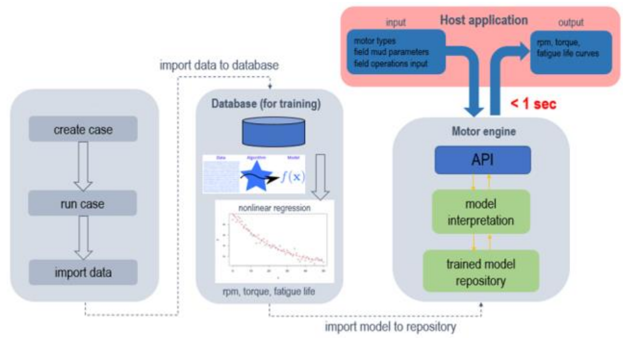

Figure 7: Motor engine scheme.

The physical model reduction enables performing required simulation for variety of operating conditions and design factors for a comprehensive portfolio of mud motors. The simulation results are used to train the machine learning algorithm, which now provides very short computation time and thus, opens the door for real-time health monitoring that will be discussed next.

4. PROGNOSTIC MODELS

The proposed PHM solution combines two different algorithms for reliable prediction of mud motor problems. It enables the estimation of motor health, both at the system level and at the subcomponent level. The description of these two PHM models and their synergistic effect for a reliable PHM solution are described below.

4.1. Subcomponent PHM model

As mentioned in section 2, the failure of power sections is the main reason of mud motor failures. Hence, power sections can be considered as the most critical subcomponent. So, the subcomponent PHM model is mainly focus on the model of the PHM model of the power section. This model enables estimating the RUL of power sections taking into account real field drilling data with significant variations in downhole conditions over time.

Fatigue characteristic of power section depends on the power section design and drilling conditions (flow rate, differential pressure, and operating temperature). Temperature is the most significant factor affecting fatigue life—the operating time of power section drops sharply with increasing temperature. For example, the fatigue life estimation for a power section operating at room temperature for a certain differential pressure and flow rate could be around 500 hours. And the same estimation for the same fixed value of differential pressure and flow rate could drop to merely 10 hours as the temperature rises to 300 degF, which is not uncommon when drilling a wellbore. From a practical point of view, drilling conditions change quite often, which means that a small timestep is needed for properly accumulating the fatigue life consumption. Thus, the ROM is vital for health monitoring.

The schematic diagram of the health monitoring approach can be found in Figure 8. The input parameters are power section characteristics, mud properties, and the drilling conditions mentioned above in the form of RT channels. At each timestep, all this information is used to estimate the consumed fatigue life.

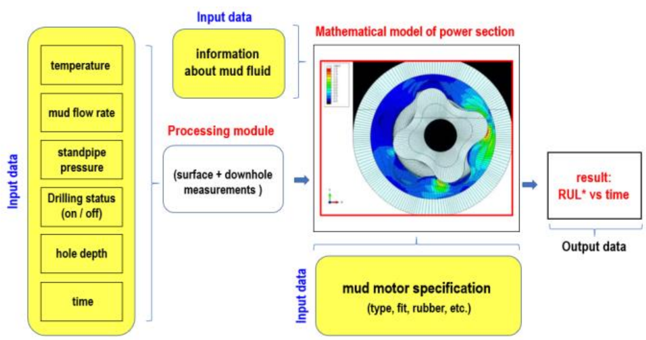

Figure 8: Scheme of prognostic algorithm for power section.

By understanding at each timestep the consumed fatigue life, one can easily integrate them to compute the remaining useful life (RUL). With the RUL available in real time, it is now possible to adjust the operating parameters depending on whether the power section is underutilized or overloaded. This enables a proper adjustment plan of operating conditions as depicted in Figure 9.

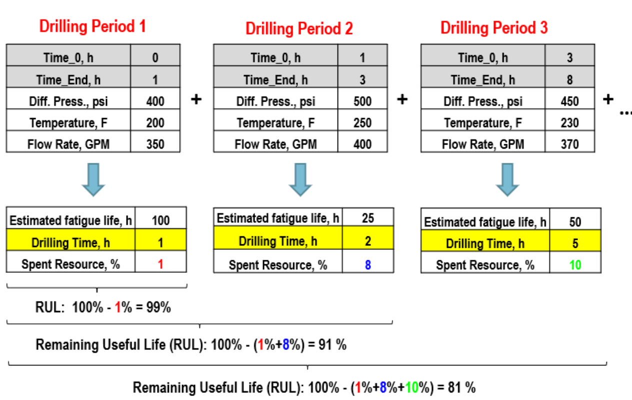

Figure 9: Managing mud motor power section performance and fatigue life by adjusting operation conditions.

Overall, current PHM workflow for power sections results in a performance boost as one can adjust the power output on the mud motor in real time and get the maximum possible ROP with informed decisions regarding the remaining useful life of the motor.

4.2. System level PHM model

As discussed in section 2, the rotational speed output of a mud motor is governed by the power curves. Figure 10 shows an example of a power curve of a power section taken from a specification sheet of a mud motor. Inside the specification sheets, curves are plotted for different rubber types, fits, temperatures, and flow rates. These curves are often generated from a mud motor dyno test or modeling of the power section as in Figure 2.

The rpm value on the power curve denotes the designed rotational speed of the power section under certain operational conditions. Under a given pumping flow rate and operating differential pressure, the mud motor should work at the designed rotational speed (red curve in Figure 10), which is referred as the nominal rpm, ω. Meanwhile, the actual mud motor output rotation speed, ω^* may have some discrepancy $\Delta\omega$ compared to the nominal rpm.

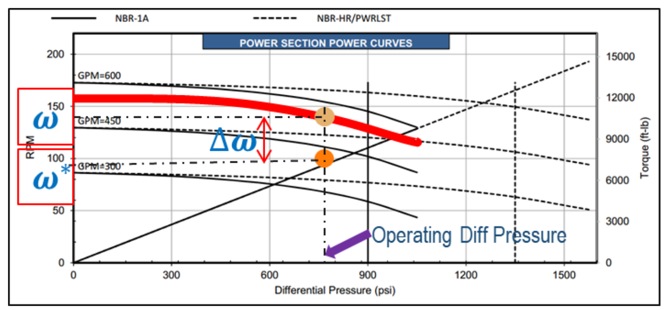

Figure 10: Power curve and definition of mud motor degradation indicator.

Due to the degradation of the mud motor, the actual mud motor rpm decreases, causing the difference to grow larger as the usage of the mud motor increases. Therefore, a mud motor degradation indicator R is defined as follows to quantify how much the mud motor has degraded.

$$R \triangleq \frac{\omega - \omega^*}{\omega} \quad (2)$$

Where the nominal rpm ω can be inferred from mud motor power curves (extracted from the power section sub-component model) and the data acquired from the surface which includes flow rate and differential pressure. The actual mud motor output rpm ω^* can be measured from downhole sensor instrumented in or below the mud motor, which is typically on the bit, rotary steerable tool, or MWD tool (Sugiura, J. et al., 2019, Sugiura, J. et al., 2021).

An example of the degradation indicator calculation from an actual field job is shown in Figure 11. At the beginning of the run, the actual mud motor output rpm was very close to the nominal rpm value, and the degradation indicator was very close to zero, indicating the mud motor was in a fresh condition. As the drilling progressed, the actual mud motor rpm started to diverge from the nominal mud motor rpm, which caused the increase of degradation indicator. Moreover, a linear regression on the degradation indicator can also be performed to evaluate the change rate of the degradation indicator. The change rate of the degradation is also a useful performance indicator when comparing across different field jobs, which enables ranking different mud motor types, bits, and operation parameters.

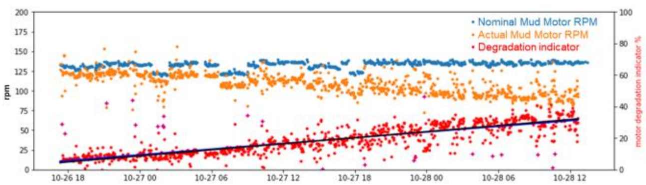

Figure 11: Mud motor nominal **rpm**, actual **rpm** and degradation indicator.

This model leverages the mud motor modeling, surface data, and downhole measurement together to evaluate the performance and health condition of the mud motor at a system level. With the degradation indicator, the model captures not only the wear on the power section, but also other factors, such as the bearing wears and leakages, which could have an impact on the mud motor rotational speed output. (Li, F., et al., 2019, Zhang, Z., et al., 2020)

4.3. Combination of the system level and subcomponent-level PHM models

The subcomponent level (power section) PHM model provides an accurate estimation of the elastomer health within the power section, which is the most critical and life-limiting component. This model enables estimating the RUL of elastomer over time. The RUL shows the serviceability of the elastomer and indicates the need to replace the power section before any physical damage to the elastomer itself. Thus, this subcomponent-level prediction complements the system-level PHM model, which mainly focus on damages that are apparent and have physical effects inside the mud motor.

At the same time, the downhole mud motor may have other reasons for failure. These can be problems with the transmission, housing, and bearing section, as well as problems with the elastomer inside the power section due to reasons other than fatigue (high vibration, abrasion). According to some statistics, such problems are the cause of approximately 40% of all downhole mud motor failures. The subcomponent power section PHM does not cover these causes, but the system-level PHM can detect those problems.

The combination of two different models enables covering almost 100% of all cases of mud motor failure and helps to avoid critical failures, as they provide accurate information about the state of the downhole mud motor over time.

5. Validation

Both models were properly tested on a large volume of field data and very good correlation was observed between predictions and real mud motor failures. A more detailed description of the validation results is provided below.

5.1. Sub-component PHM model

The subcomponent (power section) PHM model was validated both experimentally and also in the field. We validated accuracy of the modeling results used in this PHM model as well as fidelity of the PHM predictions for mud motor power sections.

Firstly, the high-fidelity modelling approach was validated experimentally using a specially designed experimental set-up. This equipment involved taking measurement of over 100 different signals, including pressure at many different locations inside the power section, temperature measurement outside the stator and inside the rubber, torque, flow rate, rpm, lateral displacements at both end of the rotor, shock and vibration at the clamped areas of the stator. More information on the validation process and other details can be found in (BA, et al., 2016).

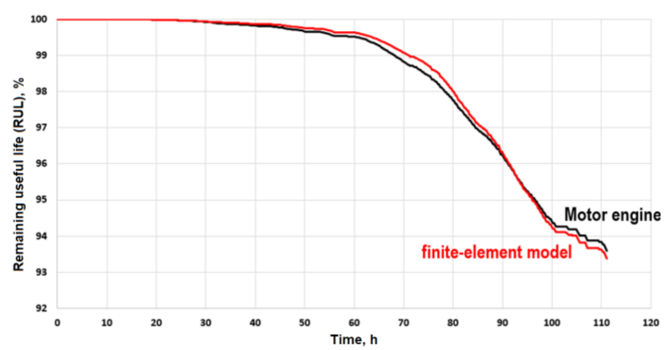

Figure 12: Cumulative remaining useful life curves from ROM (black line) compared with high-fidelity model (red line).

Secondly, the motor engine ROM needed to be validated against the high-fidelity FE model. Figure 12 depicts the comparative fatigue life curves between the FE simulation and the motor engine ROM: Fatigue life output from the FE approach shown in red, motor engine ROM fatigue life output shown in black. The matching between the two is seamless.

The entire power section PHM workflow has been evaluated on a variety of field data from various locations around the world. It has been tested on both legacy data and during recent field trials. During the field test PHM performs well after analyzing over 300 different runs with a total pumping volume of more than 13,500 hours in a fleet of more than 100 different stators in different locations with different drilling conditions, considering a variety of temperature and drilling parameters.

During the field tests, several fatigue-related field failures were experienced. For each of them, postrun data processing using the subcomponent PHM model was matching the observed life duration very well. Typical results of processed data for the cases with high probability of the mud motor failure due to elastomer fatigue can be found in Figure 13.

a

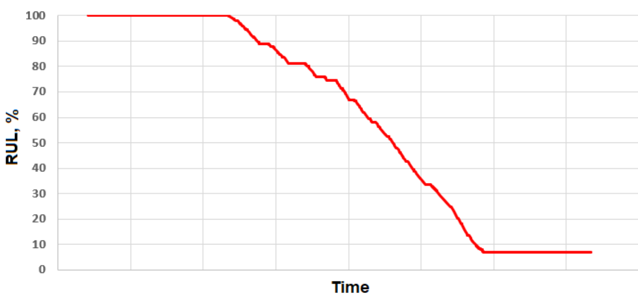

b

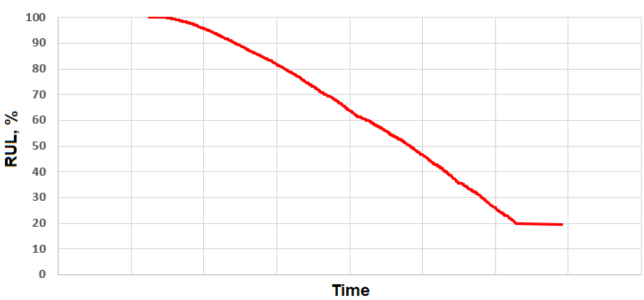

Figure 13: RUL curves for the field drilling cases with failed elastomer due to fatigue.

Figure 13a shows a case where the RUL at the end of drilling was approximately 7%, indicating a very high probability of elastomer fatigue failure. These results completely coincide with the results of visual inspection of the stator after operation—some elastomer cracks and minor chunking were found. Later analysis indicated that the wellbore temperature was higher than expected.

Figure 13b shows another case with RUL of 20% at the end of drilling job that also indicates a high likelihood of elastomer failure. This result is consistent with a postjob inspection of the stator, which shows significant elastomer chunking. Investigation of this case has shown that the power section was incorrectly selected for this well with challenging drilling conditions.

A typical RUL curve for a drilling case where the power section had a high RUL value at the end of the job is shown in Figure 14. In this case there was approximately 88% RUL after the drilling job, and this result was consistent with the visual inspection of the power section, which didn't show any elastomer damage inside the stator.

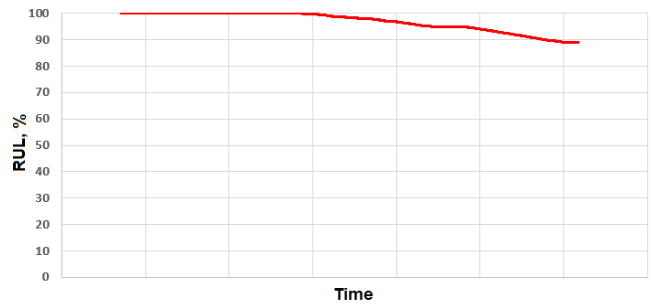

Figure 14: RUL curve for the field case with a power section without any problem after drilling job.

The accuracy of the model allowed the field test locations to build trust on the model and to start following more closely the modelling predictions. As the consequence, locations were exceeding the nominal standard fixed usage hours limit when the remaining useful life given by the PHM is high (low risk of failure due to fatigue), reducing the cost of the service delivery. And, on the other hand, to avoid a premature failure due to fatigue when the remaining useful life reach a critical (high chance of failure) level before the nominal usage hours limit in the location, they would refrain from extending the usage

At the end, there was a projected yearly savings of 25% on maintenance cost at the same time as a failure rate reduction by 10%, which was quite an achievement.

5.2. System level PHM model

The system level PHM model has been applied to a large number of field jobs and correlates well with the performance as well as the mud motor incidents captured in the field. A couple of field cases are discussed in more details and they demonstrate how the system-level PHM model can be helpful to identify potential field issues related to mud motor.

The first case is a motorized push-the-bit type RSS in the BHA. The mud motor power section was used to drive the RSS as well as deliver additional torque to the drill bit. The drilling run consisted about 3,000 ft drilled. The drilling was stopped due to a crack-induced washout at a location below the mud motor. The incident report also stated the mud motor experienced stalls during the run. After the motor was retrieved above the surface, the bit box was loose and could be rotated freely. This was a clear indication of damages occurred inside the mud motor. Figure 15 showed the nominal mud motor rpm against the actual measured mud motor rpm along with the degradation indicator that were generated by the system-level PHM model in the post job analysis. The results show that the mud motor started drilling under expected performance, also that the degradation of the mud motor accelerated with drilling time. At the end of the job, the mud motor had degraded about 40% of its designed capability. The weakening of the mud motor might have contributed to the crack-induced washout to the other component.

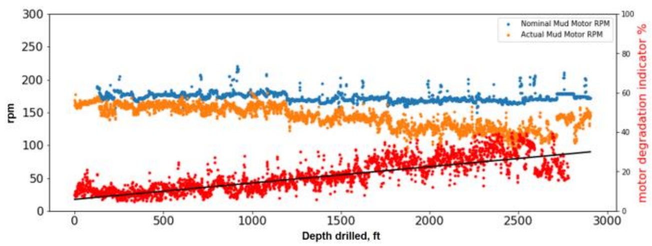

Figure 15: First case showing a drilling run of a motorized push-the-bit RSS.

The second case is also a motorized RSS BHA. The run lasted around 5,500 ft and was terminated due to mud motor dysfunction. The failure report stated that the mud motor was found to have no power output before the drilling was stopped. Figure 16 showed the processed results from the system-level PHM model. As shown from the degradation indicator, the mud motor had completely lost its capability to deliver power to the drill bit, which matched precisely the field observation. More interestingly, it was noticed that the degradation indicator had a clear change in the growth trend after drilling about 4,500 ft. When reviewing the recorded drilling data, it was found that extreme drilling parameters were applied at that time aiming to drill faster. The extreme loading accelerated the degradation of the mud motor until it entirely lost its capability. If the combination of the subcomponent level PHM model and the system-level PHM model was implemented in real time, the sharp decrease in fatigue combined with the degradation indicator would have raised a flag to change the drilling parameters; the complete destruction of the mud motor might have been avoided by the alert from the combined PHM solution.

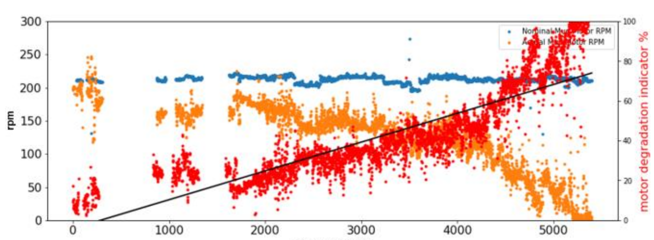

Figure 16: Second case showing a drilling run with significant mud motor degradation.

With lower degradation rate, the motor can survive longer time and drill longer distance. Figure 17 presents statistics of motor drilling distance versus degradation rate from over 500 jobs. It shows that, statistically, a motor with lower degradation rate has a better chance to reach a deeper depth.

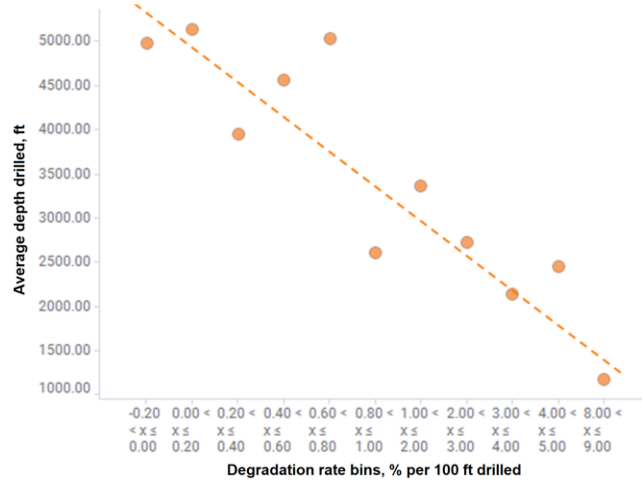

Figure 17. Average drilled depth vs. degradation rate.

5.3. Combined PHM solution

The joint work of the two PHM algorithms was tested using field data. As expected, the results showed a high reliability in predicting the possible failure of the motor, both due to the fatigue failure of the elastomer inside power section stator, and due to other reasons not related to such type of fatigue.

Figure 18 depicts a typical example where the power section PHM algorithm shows a low RUL at the end of the drilling operation (RUL = 6.9 % – top plot). After observing of such low RUL, the power section stator was sent to the shop for relining repair (replacement of the elastomer inside stator) in accordance with maintenance criteria. Postjob inspection revealed fatigue-related elastomer microdamage that could lead to the power section failure during further operation. At the same time system level PHM model didn't show any critical levels of mud motor degradation (degradation rate ~0.11 % / 100 ft – bottom plot). This is a bright example where the first model detects the motor issue, but second model doesn't.

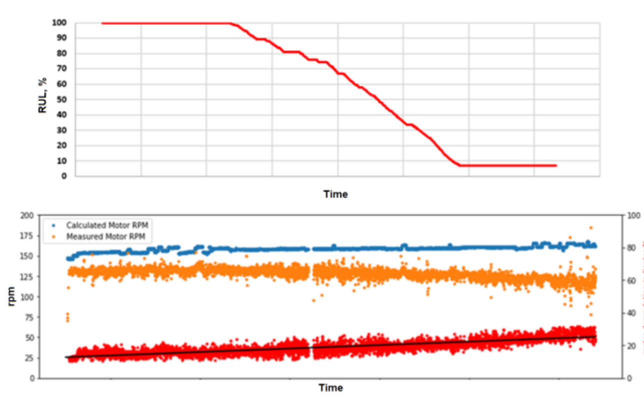

Figure 18. Comparison of the FE simulation results and the motor engine output.

Figure 19 depicts another example where system level PHM model shows a high level of mud motor degradation (degradation rate ~0.8 % / 100 ft – bottom plot), but power section PHM model does not give any inkling about problems (RUL = 63% at the end of the work – top plot). In this case, the mud motor lost differential pressure and the drive shaft was broken, so failure was not related to the elastomer fatigue.

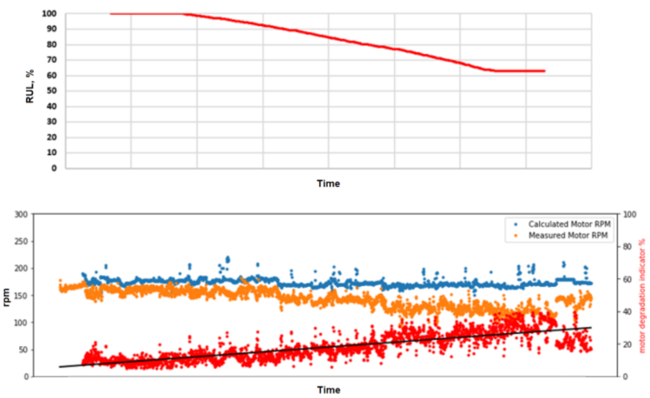

Figure 19. Comparison of the FE simulation results and the motor engine output**.**

6. Conclusion

An innovative mud motor PHM solution based on accurate PHM models has been exposed here. This PHM solution combines two different PHM models for reliable prediction of possible problems with mud motors. It enables the estimation of the mud motor health both on the system level with the entire mud motor and on the subcomponent level (power section PHM model).

The system level PHM is centered around a mud motor degradation indicator. Based on the study of large datasets, good correlation was observed between the mud motor degradation indicator and mud motor failures.

The subcomponent level PHM is grounded on a RUL prediction of the elastomer inside the power section which is the most failed component. The subcomponent PHM model was also successfully verified and tested in the field. Comparison of the predicted mud motor fatigue life with the actual observed postjob conditions and job failures demonstrated good results of the developed models.

The combined PHM solution enables the optimization of mud motor selection, drilling configuration, and maintenance operations by minimizing RUL uncertainties while facilitating rerun decisions and avoiding overmaintenance and premature retirements. The whole solution is currently being integrated into a drilling platform including the maintenance system, the well construction planning, and the execution. It maximizes the equipment usage with increased drilling performance without sacrificing reliability and enables optimal fleet management of the drilling process for both revenue maximization and sustainability.

Acknowledgement

Authors would like to thank all contributors to the project: Nikolas Davaul, Jamie Farmer, Jennifer Gilliam, Eimund Liland, Henry Massie, Benjamin Snyder, Erling Sokn and John Troncoso.

References

BA, S. et al., 2016. Positive Displacement Motor Modeling: Skyrocketing the Way We Design, Select, and Operate Mud Motors. SPE - ADIPEC, pp. 183298-MS.

Ba, S., Belov, D., Nobre, D., Yin, L., Johnson, E., 2019. Combined Data Analytics and Physics-Based Simulation for Optimum Bit, Motor, BHA Combination. (OTC-29875-MS) 2019 Offshore Technology Conference, Brasil

Ba, S. & Kolyshkin, A., Determining the life span of an elastomer in a motor. US10139326B2

Bataineh, M. & Marler, T., 2017. Neural network for regression problems with reduced training sets. *Neural Networks*, Volume 95, pp. 1-9.

Kolyshkin, A., Predicting Mud Motor Performance and Reliability with Reduced Order Modeling, in: WCCM-ECCOMAS2020. DOI: 10.23967/wccm-eccomas.2020.282URL https://www.scipedia.com/public/Kolyshkin_2021a

Li, F., Neelgund, R. V., Smith, D. L., & Blackman, W. (2019, March 22). Drilling Dynamics Measurements on Positive Displacement Motors PDM Enhance Performances and Reliability. IPTC-19498 International Petroleum Technology Conference.

Shaw, B.H.K., Ramier, J., Ba, S., Busfield, J.J.C., 2019. Characterising the Cyclic Fatigue and Static Tear Resistance of HNBR Compounds, 2019 International Conference of Rubber, London

Sugiura, J. and Jones, S. 2019. A Drill Bit and a Drilling Motor with Embedded High-Frequency (1600 Hz) Drilling Dynamics Sensors Provide NewInsights into Challenging Downhole Drilling Conditions. SPE Drill & Compl 34 (3): 223–247. SPE-194138-PA. https://doi.org/10.2118/194138-PA.

Sugiura, J. and Jones, S. 2021. Measurement of Mud Motor Back-Drive Dynamics, Associated Risks, and Benefits of Real-Time Detection and Mitigation Measures. SPE Drilling & Completion (2021), SPE-204032-PA. https://doi.org/10.2118/204032-PA

Tiraspolsky, W., Hydraulic Downhole Drilling Motors: Turbo Drills and Positive Displacement Rotary Motors. Houston: Houston Gulf Publishing Co. (1985).

Zhang, Z., Shen, Y., Chen, W., and Chen, Z., 2020. Analyzing Energy and Efficiency of Drilling System with Mud Motor through Big Data. SPE-201502 SPE

Annual Technical Conference and Exhibition. https://doi.org/10.2118/201502-MS.

BIOGRAPHIES

Dmitry A. Belov received his Ph.D. degree in Applied Mechanics from the Faculty of Physics and Mechanics in St. Petersburg State Polytechnical University, Russia in 2009. He joined Schlumberger in 2008 as a research scientist and since that time change several positions inside this company including physicist, modeling & simulation engineer and data scientist. Currently, he is working as a data scientist in Katy, TX and responsible for development of the new PHM algorithms for drilling equipment. His expertise is numerical modelling of Multiphysics (acoustics, ultrasonic, composite materials, elastomers, strength, etc.), data analysis and analytics as well as software development for data processing.

Zhengxin Zhang received his M.S. degree in Mechanical Engineering from Texas A&M University in 2010. He is also a licensed professional engineer on the Texas Board of Professional Engineer. He joined Schlumberger in 2011 and is currently working as a senior engineer on drilling system modeling, drilling dynamics interpretation, data analytics and drilling software development.

Yuelin Shen received his Ph.D. degree in Mechanical Engineering from the Missouri University of Science and Technology in 2002. He is currently a Technology Advisor in Schlumberger, working on drilling system modeling, drilling dynamics interpretation, drill bits and drilling tools engineering.

Wei Chen received his Ph.D. degree in Mechanical Engineering from Northwestern University in 2009. He joined Schlumberger in 2010 and is currently working as Principal Engineer in drilling software development group. His expertise includes drilling system modeling, drilling dynamics interpretation, and drilling data analysis.

Samba Ba received a first master’s degree from the Ecole Polytechnique in France in 2001. He also holds a diplome des Grandes Ecoles from the Ecole National des Ponts et Chaussees and a DEA from the University Pierre et Marie Curie in Paris VI. He has worked in the field for the Drilling and Measurement segment as MWD, LWD, and then DD up to 2006, before joining Schlumberger Cambridge Research Center as a research scientist. He then worked as a project Manager at the Schlumberger Motor Center of Excellence in Katy. Currently, he is the DrillOps Domain solution architect, working in Beijing, China.

Anton Kolyshkin received his Ph.D. in Physical Chemistry from Institute of Technical Chemistry at Russian Academy of Science in 2005. He started working in Schlumberger in 2006 in mud motor stator manufacturing and elastomer development in 2006. Currently he works in the projects related to new elastomers and adhesives for mud motors, developing new modeling approaches and software, hyperelastic, viscoelastic and fatigue characterization.

Sergio D. Rocchio received his Electronic Engineer degree in 2009 from the Faculty of Exact Sciences and Technology in the National University of Tucuman, Argentina. He joined Schlumberger Argentina operations base in 2010 as a full time ME; in 2013 was assigned as Maintenance Supervisor for Macueta, Pan American project; in 2014 was assigned as SQE for ABC geo-market; in 2016 he was assigned as GME for Argentina; in 2018 was transferred to Katy Technology Center (USA) to his current assignment as a Service Quality Expert. His expertise is in failure investigations, field operations and maintenance.

Daniel E. Viassolo is a Data Analytics Manager and Principal Data Scientist with the Well Construction Division, Schlumberger, based in Houston, TX. He is a technical expert in Prognostics & Health Management, Machine Learning, Optimization, and Control Systems. Daniel authored 27 granted US patents and more than 40 papers while working on diverse applications across Oil & Gas, Renewable and Conventional Power Generation. He obtained a PhD (Purdue University) and attended Business leadership training (Texas A&M).